Journal of the Iranian Chemical Society (2023) 20:97–107
https://doi.org/10.1007/s13738-022-02656-y

ORIGINAL PAPER

Copper 4-chlorobenzoate with isonicotinamide: synthesis, crystal structure, optical characterization and anticancer and cytotoxic properties

Alpaslan İşkey[1] · Füreya Elif Öztürkkan[2] · Giray Buğra Akbaba[3] · Mustafa Sertçelik[2] · Tuncer Hökelek[4]

Received: 27 May 2022 / Accepted: 28 August 2022 / Published online: 9 September 2022

Abstract
In this study, a new metal complex, bis(μ-4-chlorobenzoato-κ^2O:O′)bis[(4-chlorobenzoato-κ^2O:O′-bis(isonicotinamide-κN) copper(II)] (**1**), was synthesized. The crystal structures of the complex were determined by single-crystal XRD. In addition, the structure was characterized by elemental analysis and FTIR spectroscopy. The intermolecular interactions of the complex were determined by Hirshfeld surface analysis. The optical and fluorescence properties of the complex were recorded with the help of UV–Vis and fluorescence spectrophotometer. In addition, the anticarcinogenic effects of the complex on DLD-1, MCF-7 and PC-3 cell lines and their cytotoxic properties on human lymphocyte cells were investigated by (3-(4,5-dimethylthiazol-2-yl)-2,5-diphenyltetrazolium bromide (MTT) method. The complex has a dimeric structure. The intermolecular interactions that contribute the most to the crystal structure are H···H, O···H/H···O and H···C/C···H interactions. The complex was exhibited broad emission peaks between 350 and 550 nm. It was determined that the complexes did not cause cytotoxic effects on lymphocyte cells. Complex 1 caused a strong cytotoxic effect on DLD-1 colon cancer cells. The complex was determined to cause low cytotoxicity on MCF-7 and PC-3 cells. The interactions of the complex with synthetic DNA dodecamer were investigated by molecular docking. It has been determined that the complex inhibits these proteins through hydrophobic, electrostatic and non-covalent interactions.

Keywords 4-Chlorobenzoic acid · Copper complex · Fluorescence · MTT assay · Anticancer · Molecular docking

Introduction

Cancer is a disease that occurs when cells divide rapidly and uncontrollably in the tissues and usually results in death [1]. Although many methods are used in cancer treatment, chemotherapy, which uses various natural and synthetic compounds that have the potential to inhibit or control the proliferation of cancerous cells, is the main treatment method [2, 3]. Although medicinal chemistry relies almost entirely on organic compounds and natural products, over the past three decades metal complexes have been used as pharmaceutical agents such as diagnostic agents or chemotherapeutic drugs [4]. Molecules containing metals as therapeutic agents are much more effective than free organic compounds. The pharmaceutical properties of metal-based drugs can be changed by the coordination number, geometry and redox ability of the metal [5–7]. Cisplatin, which is prescribed to the vast majority of cancer patients, is considered one of the most important drugs in cancer treatment [1, 8]. Despite its treatment success, cisplatin's clinical use has been limited in recent years due to its side effects, high toxicity and acquired resistance. These limitations have accelerated the research and development activities of alternative metal-based drugs that contain metal ions other than platinum, provide alternative mechanisms of action and may

✉ Füreya Elif Öztürkkan
fozturkkan36@gmail.com

Mustafa Sertçelik
mustafasertcelik@gmail.com

[1] Department of Chemistry, Kafkas University, Kars, Turkey

[2] Department of Chemical Engineering, Kafkas University, Kars, Turkey

[3] Department of Bioengineering, Kafkas University, Kars, Turkey

[4] Department of Physics, Hacettepe University, Ankara, Turkey

have enhanced anticancer activity [9]. Non-platinum-based compounds also include copper complexes [10].

An essential element for humans and most aerobic organisms, copper is important for the function of many enzymes and proteins [7, 11, 12]. Many studies have reported that copper complexes are less cytotoxic to normal cells when compared to a nonessential metal such as platinum [13–15]. Low toxicity is one of the most important parameters in drug design. It has been reported that copper compounds and their complexes with N-donor ligands have biologically active properties such as antioxidant [16], antitumoral [17], antifungal [18] and antibacterial [19]. The toxicity of copper is attributed to its ability to generate reactive oxygen species (ROS), replace other metal ions, peroxidize lipids and directly degrade DNA and RNA. It has been reported in previous studies that copper complexes cause anticarcinogenic effects on various human cancer cells such as prostate, breast, colon, lung and brain [10, 20]. Copper is a necessary and appropriate element for living things. Copper and its complexes were highly effective against viruses, bacteria, yeasts and fungi. The selective permeability of cancer cell membranes causes copper to accumulate in tumors. Many copper complexes have been suggested as anticarcinogenic drugs based on the findings of both in vitro and in vivo studies [21]. Copper complexes with nitrogen donor ligands such as thiosemicarbazone, purine, imidazole and benzohydroxamic acid have been reported as anticancer agents against various cancer cell lines. However, there is no anticancer study of copper aryl carboxylate complexes of pyridine derivatives such as nicotinamide and isonicotinamide [22–24]. While some copper complexes have antiproliferative effects on cancer cell lines, most of them have cytotoxic effects. For example, copper 5 methoxyisatin thiosemicarbazone complexes exhibited antiproliferative activity against MCF7, A549, HeLa and HEK 293 cell lines [25]. Thiosemicarbazone-copper(II) complexes caused 70% cell death against the U937 cell line [26]. Copper 8-hydroxyquinoline thiosemicarbazone complexes were cytotoxic to human non-small cell lung cancer (NSCLC) cell lines A549, MCF7 and human MSTO mesothelioma cell lines [27]. In this study, bis(μ-4-chlorobenzoato-κ^2O:O′)bis[(4-chlorobenzoato-κ^2O:O′-bis(isonicotinamide-κN)copper(II)] was synthesized and characterized by single-crystal X-ray diffraction, elemental analysis, FTIR spectroscopy. The optical and fluorescence properties of the complex were determined. The anticarcinogenic effects of the complex on DLD-1 colon cancer, MCF-7 breast cancer and PC-3 prostate cancer cell lines and their cytotoxic properties on human normal peripheral blood cells (lymphocytes) were evaluated by MTT method. In addition, the interactions of the complex with the synthetic DNA dodecamer target (PDB Code: 1BNA) assessment were made by molecular docking studies.

Experimental

Reagents

For sodium bicarbonate, copper(II) sulfate pentahydrate, 4-chlorobenzoic acid and isonicotinamide were purchased from Sigma-Aldrich (Germany). Phosphate-buffered saline solution, Dulbecco's modified Eagle medium (DMEM, for DLD-1, MCF-7 and PBMC cells line), dimethylsulfoxide and fetal bovine serum (FBS) (Sigma-Aldrich, Germany), RPMI 1640 (NutriCulture, Turkey for PC-3 cell line), and 3-(4,5-dimethylthiazol-2-yl)-2,5-diphenyltetrazolium bromide (MTT) and penicillin/streptomycin (Thermo Fisher Scientific) used for the determination of anticancer properties were purchased commercially. MCF-7 cells (ATCC-HTB22), DLD-1 (ATCC-CCL-221) and primary peripheral blood mononuclear cells (PBMC) (PCS-800-011) were cultured in DMEM-high glucose supplemented with 10% (v/v) fetal bovine serum and 1% penicillin/streptomycin (ThermoFisher) at 37 °C with 5% CO_2. PC-3 cells (ATCC CRL-1435) were cultured in RPMI-1640 supplemented with 10% (v/v) fetal bovine serum and 1% penicillin/streptomycin (ThermoFisher) at 37 °C with 5% CO_2. Gemcitabine and 5-fluorouracil which are reference drugs were purchased from Lilly and Kocak Farma, respectively.

Instrumentation

Elemental analysis for C, H and N was carried out on a LECO CHNS 932 elemental analyzer. FTIR spectra were recorded from solid samples in the wavelength range of 4000–600 cm^{-1} using Perkin-Elmer Frontier™ FTIR spectrometer with ATR detector. UV–Vis spectra were recorded with a Thermo Scientific Evolution Array model UV–Vis spectrophotometer from solutions at a concentration of 0.01 mg/mL in the wavelength range of 190–1100 nm. Fluorescence spectra were measured with Agilent Cary Eclipse Fluorescence Spectrophotometer device from samples at a concentration of 0.01 mg/mL in the wavelength range of 190–1100 nm. Hed Lab X BIO MSC CLASS II Biosafety cabinet, Thermo Fisher EVOS FL Inverted Microscope, Panasonic MCO-170AICUVH-PE CO_2 Incubator and BioTek Epoch UV–Vis Spectrophotometer were used in cytotoxicity and anticancer studies.

X-ray crystallography

The crystallographic data of the title compound were collected on a Bruker APEXII CCD area-detector

Scheme 1 Schematic illustration of the synthesis of the complex

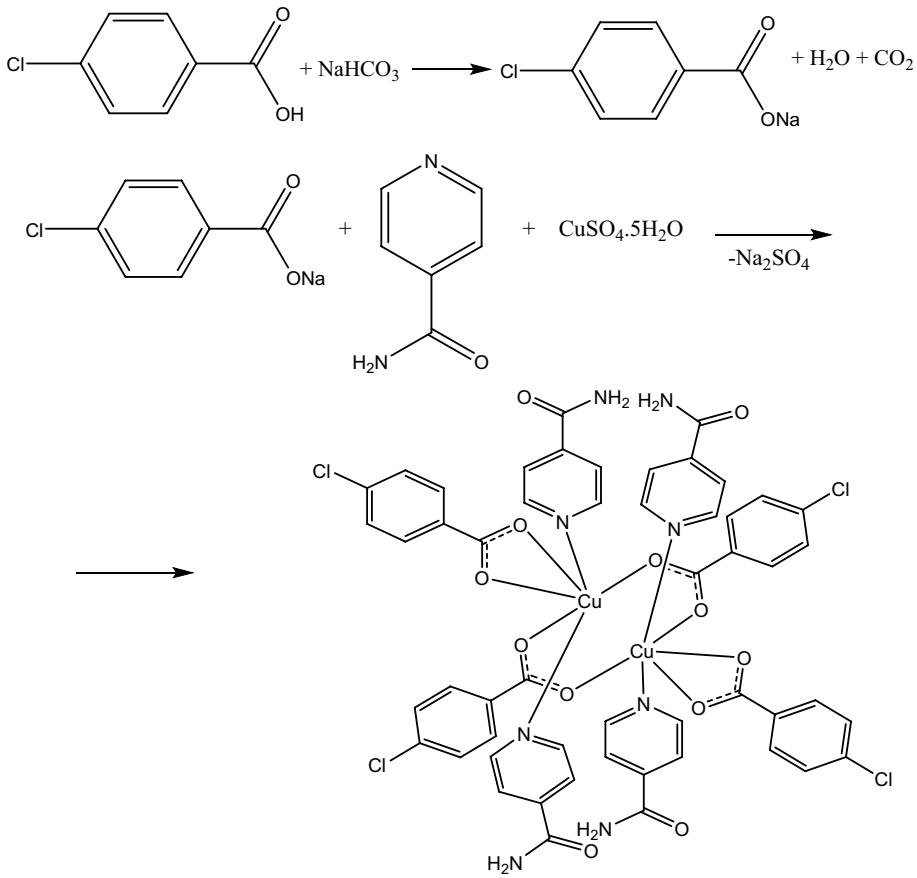

diffractometer by Mo K_α radiation. The multi-scan absorption correction (*SADABS*; [28]) applied data were processed by SHELX program packages (*SHELXS97* and *SHELXL97* [29]) for solving and refining the structures, and ORTEP-3 [30] and PLATON [31] programs were used in drawings. The H atom positions were calculated geometrically at a distance of 0.93 Å (for aromatic CH) and 0.86 Å (for NH_2) and refined using a riding model by applying the constraint of 1.2 Ueq (carrier atom) for Uiso(H) values.

Synthesis of Bis(μ-4-chlorobenzoato-κ^{2}O:O′)bis[(4-chlorobenzoato-κ.^{2}O:O′-bis(isonicotinamide-κN) copper(II)] (1)

For the synthesis of sodium 4-chlorobenzoate, sodium bicarbonate (0.84 g, 10 mmol) and 4-chlorobenzoic acid (1.56 g, 10 mmol) were mixed in 100 mL of distilled water by heating until CO_2 gas was removed. The solution of isonicotinamide (1.22 g, 10 mmol) in 20 mL of water and $CuSO_4.5H_2O$ (1.25 g, 5 mmol) in 20 mL of water were added to the prepared sodium 4-chlorobenzoate (1.78 g, 10 mmol), respectively. The mixture was filtered and left at room temperature, blue crystals formed within a week. Yield: 86.69% (2.67 g). Anal. calc. for $C_{52}H_{40}C_{l4}Cu_2N_8O_{12}$: C, 50.29; H, 3.57; N, 9.02%. Found: C, 50.91; H, 3.43; N, 9.23%. Selected IR bands (cm^{-1}): ν(NH)as 3379, ν(NH)s 3163, $\nu(C–H)_{as}$ 3050, $\nu(C–O)_{carboxamide}$ 1686, $\nu(COO^-)_{as}$ 1571, $\nu(COO^-)_s$ 1388, $\nu(C–C)_{INA}$, $\nu(C\text{-}N)_{INA}$ 1030, δ(C–Cl) 857. UV–Vis spectra (nm) 282, 753 (Scheme 1).

Hirshfeld surface analysis

Hirshfeld surface analysis has been widely used in recent years to investigate intermolecular interactions. For a visual representation of the intermolecular interactions of the synthesized complex, Hirshfeld surface analysis [32, 33] was performed with the CrystalExplorer 21 program [34]. The Hirshfeld surface, d_{norm} and curvature map and shape index [34, 35] and 2D fingerprint graphs [33] were obtained using the crystallographic information file (.cif) of the complex.

Determination of anticancer and cytotoxic properties

Anticancer properties of the synthesized complex on the colon (DLD-1), breast (MCF-7) and prostate (PC-3) cell lines 3-(4,5-dimethylthiazol-2-yl)-2,5-diphenyltetrazolium bromide (MTT) method were investigated. In addition, cytotoxic properties of human peripheral blood cells (PMBC) were investigated. Working concentrations are 1000; 500;

250; 125; 62.5; 31.25; 15.63; 7.81 ppm. The synthesized complex was found to be stable at room temperature and insoluble in solvents such as CCl_4 and $CHCl_3$, weak soluble in EtOH and MeOH and soluble in $(CH_3)_2CO$, DMSO, DMF and H_2O. Dimethylsulfoxide (DMSO) was used to prepare the solutions. Anticancer and cytotoxic properties were compared with starting ligands (4-chlorobenzoic acid and isonicotinamide). To apply the MTT method, 100 µL of culture medium was added to the 96-well microplates; 100 µL (5000 cells) cells were seeded into each well. The microplates were incubated for 24 h in an incubator at 37 °C and 5% CO_2, allowing the cells to adhere to the surface. Then, the samples to be tested were added to the wells containing the culture medium in 100 µL portions of each concentration. It was incubated at 37 °C for 24 h in a 5% CO_2 incubator. After incubation, 10 µL of MTT reagent prepared in PBS at a concentration of 5 mg/mL was added to each well. It was incubated for 3–4 h at 37 °C in a 5% CO_2 incubator. As a result of incubation, formazan formed in the cells was seen as purple crystals at the bottom of the wells. The culture medium was completely removed from the wells and 200 µL of DMSO was added. After 18 h of incubation, purple-colored solutions were seen depending on the viable cell density. The absorbance of the microplates was measured with the aid of a spectrophotometer at a wavelength of 570 nm [36]. Cell viability was determined by comparing the cell with the control group. The cell control group contains 100 µL of cells and 100 µL of culture medium. The cell viability of the cell control group is 100%.

Statistical analysis

The data obtained from tests were analyzed with IBM SPSS statistics for Windows package program (v.18.0, IBM Corp., Armonk, New York, USA). Two-way ANOVA (Tukey) was used to evaluate whether any treatment significantly differed from the control or each other's. Statistically significance level was accepted at % 95 ($p < 0.05$).

Molecular docking analysis

Autodock Vina program [37] was used to calculate the binding energy of the complex. The pdb file of synthetic DNA (d(CGCGAATTCGCG), PDB code 1BNA [38]) with a resolution factor of 1.90 Å was downloaded from the RCSB Protein Data Bank (https://www.rcsb.org). The crystallographic information file (.cif) of the complex was used for use as a ligand. The proteins to be modeled were optimized with BIOVA Discovery Studio Visualizer 2021 [39]. AutoDockTools 1.5.7 program [37] was used to interact with the complex and DNA molecule in the active site and to view the ligand–protein interactions. The presence of water molecules in the protein structure was eliminated, and polar hydrogens and Kollman charges were added. The root of each ligand molecule is recognized automatically, and torsions are chosen. The torsions of the ligand were allowed to rotate, and the chosen residues were analyzed. The ligands were docked in a random order to analyze where they would selectively bind. The BIOVA Discovery Studio Visualizer 2021 was used to determine the amino acids in the active site of 1BNA. Grid maps with dimensions of $72 \times 72 \times 122$ ($80 \times 68 \times 82$) and a grid-point spacing of 0.375 were generated around the center of 1BNA to contain the whole structure. The Lamarckian genetic algorithm was utilized as a docking engine, with all docking settings set to default. BIOVA Discovery Studio Visualizer 2021 [39] was used for visualization processes.

Results and discussion

Crystal structure descriptions

The crystal data and data collection information are given in Table 1. The complex's asymmetric unit contains just one-half of the complex molecule (Fig. 1). The dimeric complex consists of a binuclear Cu complex bridged by oxygen atoms of two carboxyl groups of 4-chlorobenzoate (CB) anions, where the two bidentate-bridging CB anions, one chelating CB anion and two monodentate isonicotinamide (INA) ligands coordinate to one Cu^{II} cation with a distorted octahedral geometry. The distance between Cu1 and Cu1i is 4.242 (4) (symmetry code: (i) $-x+1, -y+1, -z+1$). The sum of the bond angles O1–Cu1–O2 [53.90 (11)°], O1–Cu1–O6 [82.21 (10)°], O2–Cu1–O3 [97.45 (12)°] and O3–Cu1–O6 [120.13 (10)°] in the basal plane around CuII cation is 353.69 (11)°. This supports the presence of CuII cation, although with a very minor deviation from the basal plane, where the CuII ion is 0.1020(3) Å less than the best least-squares plane of the four O atoms (O1, O2, O3 and O6) [with a maximum deviation of −0.103 (3) Å for atom O1]. With an average Cu1–O bond length of 2.2245 (30), the four O atoms surrounding the Cu1 atom generate a distorted square-planar geometry (Table 1, Figs. 1 and 2). The slightly distorted octahedral coordination around the copper atom is completed via the pyridine nitrogen atoms of the INA ligands, and the Cu-N1 and Cu-N3 bond lengths are 2.049 (3) Å and 2.033 (3) Å, respectively (Table 1, Figs. 1 and 2). On the other hand, the Cu^{II} cation is 0.2405 (3) Å and 0.2426(3) Å below and above the best least-squares planes of the carboxylate, (O1/O2/C1) and (O3/O6/C8), groups, respectively. The near distances values of the C1–O1 [1.260 (4) Å], C1–O2 [1.236 (4) Å] and C8–O3 [1.288 (4) Å], C8i–O6 [1.237 (4) Å] bonds in the carboxylate groups were supported delocalized bonds, rather than localized single and double bonds (symmetry code: (i) $-x+1, -y+1, -z+1$).

Table 1 Experimental details

Crystal data	
Chemical formula	$C_{52}H_{40}Cl_4Cu_2N_8O_{12}$
M_r	1237.82
Crystal system, space group	Triclinic, $P-1$
Temperature (K)	296
a, b, c (Å)	8.9824 (2), 11.7482 (3), 13.2904 (4)
α, β, γ (°)	88.321 (4), 83.440 (3), 72.321 (3)
V (Å^3)	1327.49 (6)
Z	1
Radiation type	Mo $K\alpha$
μ (mm^{-1})	1.07
Crystal size (mm)	0.45 × 0.30 × 0.25
Data collection	
Diffractometer	Bruker *APEX*II CCD
Absorption correction	Multi-scan *SADABS*; Bruker, 2012
T_{min}, T_{max}	0.38, 0.77
No. of measured, independent and observed [$I > 2\sigma(I)$] reflections	31,946, 6671, 5562
R_{int}	0.057
$(\sin \theta/\lambda)_{max}$ (Å^{-1})	0.671
Refinement	
$R[F^2 > 2\sigma(F^2)]$, $wR(F^2)$, S	0.083, 0.255, 1.10
No. of reflections	6671
No. of parameters	352
H atom treatment	H atoms treated by a mixture of independent and constrained refinement
$\Delta\rho_{max}$, $\Delta\rho_{min}$ (e Å^{-3})	1.82, −2.69
CCDC number	2,160,665

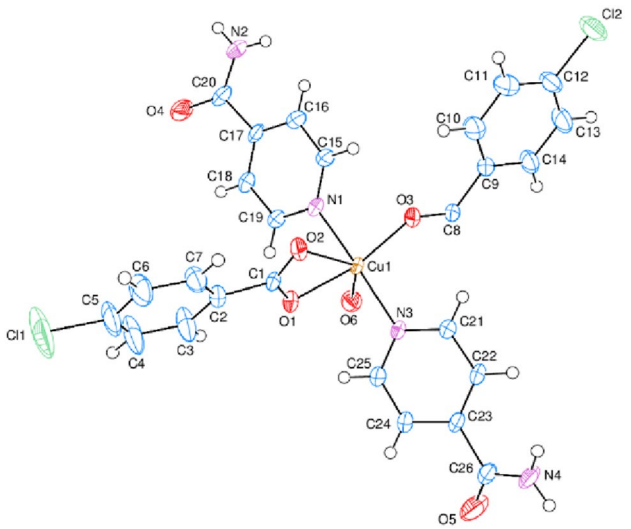

Fig. 1 The asymmetric unit of the complex with the atom numbering scheme. Thermal ellipsoids are drawn at the 50% probability level

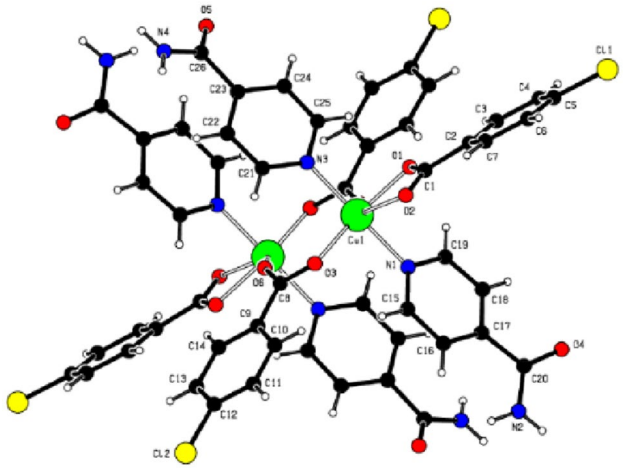

Fig. 2 The molecular structure of the complex with the atom numbering scheme [symmetry code for the unlabelled atoms is $-x+1, -y+1, -z+1$]

The O1–C1–O2 [123.7 (3)°] and O3–C8–O6i [123.6 (3)°] bond angles seem to be increased compared to that present in a free acid [122.2°]. The corresponding values for these angles in the closely related structures are 125.2(3)° in $[Cu(C_7H_6NO_4S)_2(C_6H_6N_2O)_2(H_2O)]$ [(I); [40], 123.5(2)° and 120.4(2)° in $[Zn(C_7H_5O_3)_2(C_6H_6N_2O)_2]$ [(II); [41], 125.2(5)° in $[Mn(C_7H_4ClO_2)_2(C_{10}H_{14}N_2O)_2(H_2O)_2]$ [(III); [42] and 124.3 (2)° in $[Zn(C_7H_4BrO_2)_2(C_6H_6N_2O)_2(H_2O)2]$ [(IV); [43]; the benzoate ions are coordinated to the metal atoms only monodentate in (I), (III) and (IV), and both monodentate and bidentate in (II). Within the binuclear molecule, the benzene [A (C2-C7) and B (C9-C14)] and pyridine [C (N1/C15-C19) and D (N3/C21-C25)] rings are oriented at dihedral angles of A/B = 26.31(14)°, A/C = 78.37(11)°, A/D = 70.02(11)°, B/C = 70.62(12)°, B/D = 58.35(11)° and C/D = 13.67(10)°. The dihedral angles between the planar carboxylate groups (O1/O2/C1) and (O3/O6/C8) and the adjacent benzene [A (C2-C7) and B (C9-C14)] rings are 9.72(30)° and 21.08(15)°. The O1–Cu1–O2 angle is 53.90 (11)°. The corresponding O–M–O (where M is a metal) angles are 58.3 (3)° in $[Zn_2(C_{10}H_{14}N_2O)_2(C_7H_5O_3)_4]0.2H_2O$ [44], 60.03 (6)° in $[Zn(C_9H_{10}NO_2)_2(C_6H_6N_2O)(H_2O)_2]$ [45], 52.91 (4) and 53.96 (4) ° in $[Cd(C_8H_5O_3)_2(C_6H_6N_2O)_2(H_2O)].H_2O$ [46] and 55.2 (1)° in $[Cu(Asp)_2(py)_2]$ (where Asp is acetylsalicylate and py is pyridine) [47]. In the crystal structure, the $N–H_{INA}\cdots O_{Carbx}$, $N–H_{INA}\cdots O_{INA}$, $C–H_{Carbx}\cdots O_{INA}$ and $C–H_{INA}\cdots O_{Carbx}$ [INA = isonicotinamide, and Carbx = carboxylate] hydrogen bonds (Table 2, Fig. 3) link the molecules into a three-dimensional architecture, in which they may be effective in the stabilization of the structure. There is not any C–H··· π interaction observed.

Table 2 Hydrogen bond geometry (Å, º)

D–H···*A*	*D*–H	H···*A*	*D*···*A*	*D*–H···*A*
N2–H2*A*···O2^{i}	0.86	2.21	3.027 (4)	158
N4–H4*A*···O4^{ii}	0.86	2.10	2.912 (4)	158
N4–H4*B*···O2^{iii}	0.86	2.14	2.889 (4)	145
C4–H4···O5^{iv}	0.93	2.36	3.264 (7)	165
C22–H22···O2^{iii}	0.93	2.55	3.439 (4)	161

Symmetry codes: (i) $-x+1,-y+1,-z$; (ii) $x+1, y, z+1$; (iii) $-x+2,-y+1,-z+1$; (iv) $-x+1,-y+2,-z+1$

Hirshfeld surface analysis

With Hirshfeld surface analysis, visual graphics are obtained by presenting intermolecular interactions and short or long contacts with different colors and color intensity. The red and blue surfaces seen in the d_{norm} maps of the complex represent distances shorter (close contact) or longer (distant contact) than the van der Waals radius, respectively. Also, the white surfaces show the distance equal to the sum of the van der Waals radii. It is seen that especially long distances, that is, different contacts, are more dominant in the d_{norm} maps of the complexes. In the d_{norm} map of the complexes, three-dimensional Hirshfeld surfaces were determined in the range of − 0.4990 to 1.4988 a.u (1) [33].

The adjacent red and blue triangles in the shape indices of the complexes (Fig. 4b) confirm the existence of C-H···π interactions and π-π stackings between aromatic rings (benzene and pyridine) in the crystal structure of the complex [33, 35]. The broad and flat green regions on the curvedness maps of the complexes represent a relatively flat (i.e., planar) surface area, while the blue regions indicate areas of curvedness. The flat regions around the rings on the Hirshfeld surface are attributed to the existence of π–π stackings. The 2D fingerprint plots for all interactions (Fig. 5) and the distribution of these interaction percentages are given in Fig. 6. The most important interactions are H···H (29.2%, de + di ~ 2.36 Å) interactions due to the abundance of hydrogen on the molecular surface. The second largest contribution to the Hirshfeld surface of the complex is the H···O/O···H (20.2%, de + di ~ 1.98 Å) interactions. These interactions result from the O–H···O hydrogen bonds found in the structures of the complexes as determined by single-crystal X-ray analysis. The third most important interaction is the H···C/C···H (de + di ~ 1.88 Å) interactions. These interactions confirm the C–H···π interactions and π-π stackings determined in the crystal structure analysis. In the two-dimensional

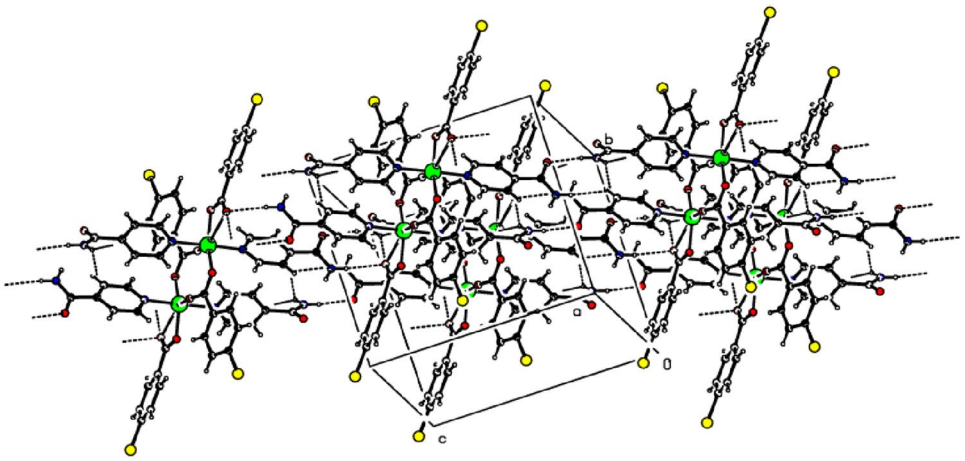

Fig. 3 A partial packing diagram. N–H_{INA}···O_{Carbx}, N–H_{INA}···O_{INA}, C–H_{Carbx}···O_{INA} and C–H_{INA}···O_{Carbx} [INA = isonicotinamide, and C_{arbx} = carboxylate] hydrogen bonds are shown as dashed lines

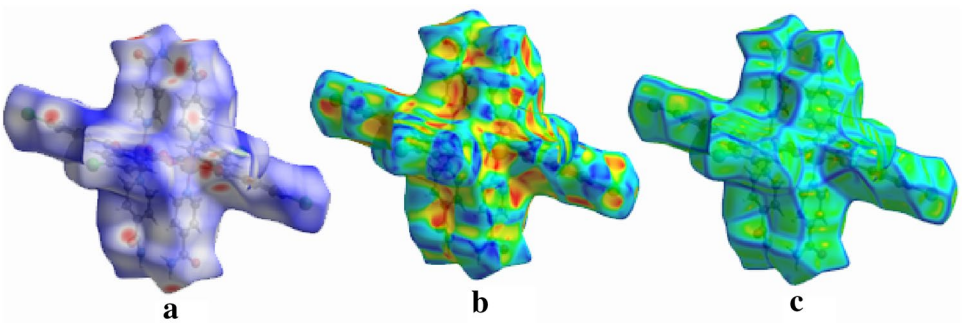

Fig. 4 d_{norm} map (**a**), shape index (**b**) and curvedness map (**c**) of the complex

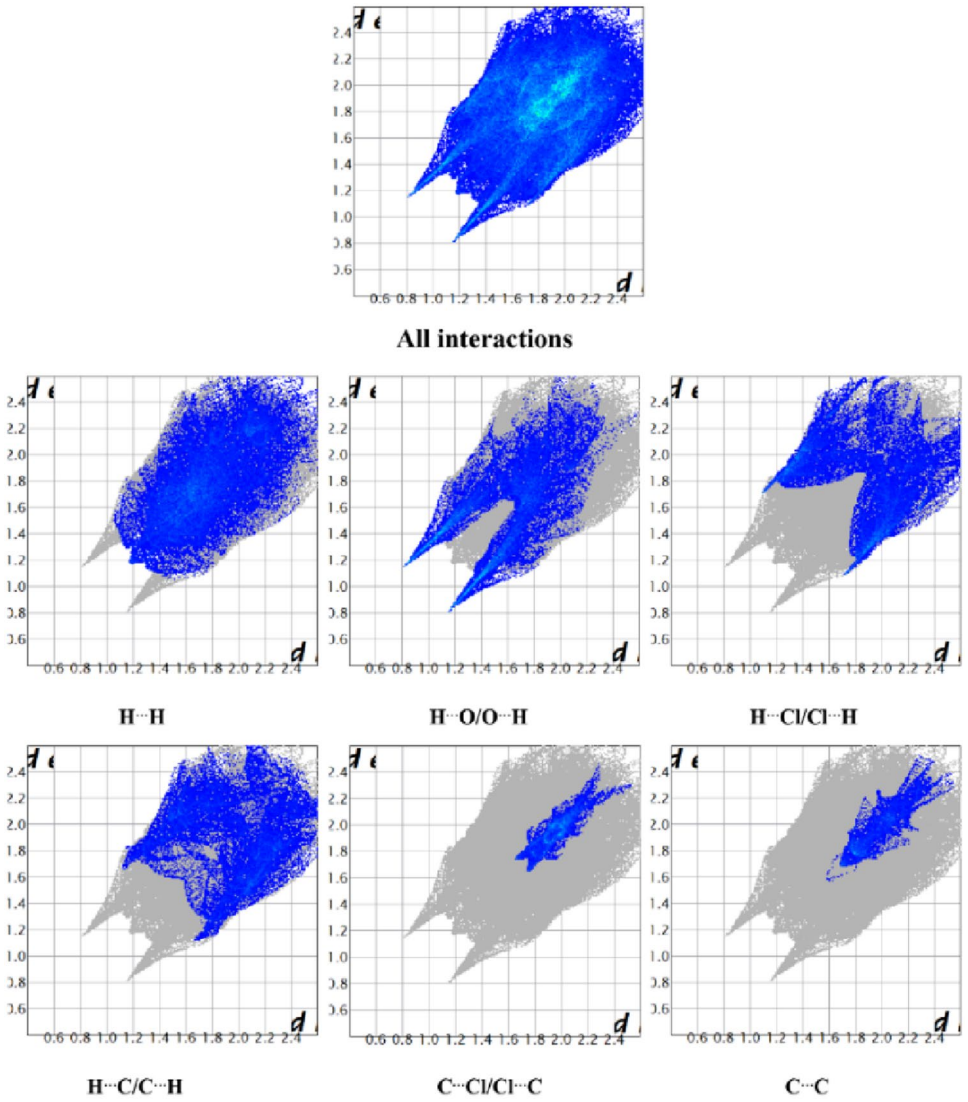

Fig. 5 2D fingerprint plots of the complex

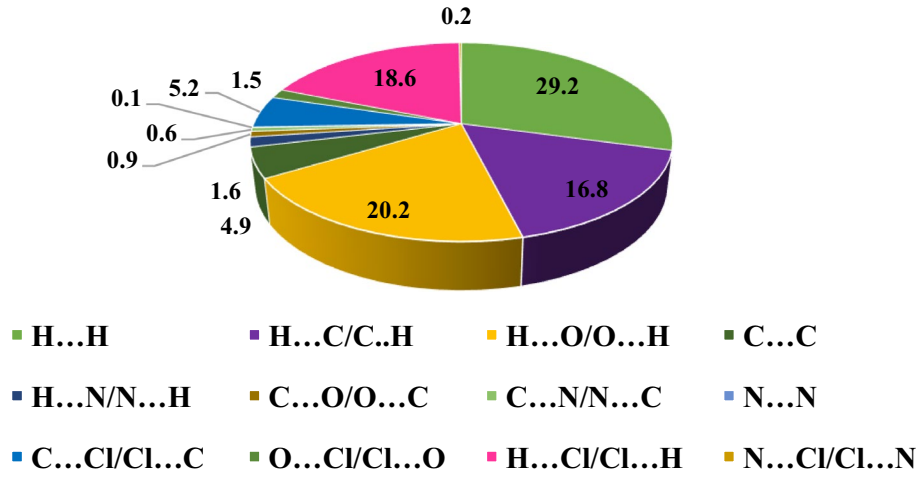

Fig. 6 The intermolecular interaction percentages of the complex

fingerprint graphs, low contribution interactions such as C···C, H···N/N···H C···O/O···C, C···N/N···C, N···N, C···Cl/Cl···C, O···Cl/Cl···O and N···Cl/Cl···N interactions were also found.

The interaction of atoms presents inside Hirshfeld surface with all atoms present in Hirshfeld surface's surroundings is determined for further research of molecular packing [48–52]. With a percentage contribution of 54.75%, our analysis suggests that the H···All interactions are the strongest interaction. According to Figure S1, the other interactions of this type are C···All, Cl–All, O···All and N–All, with percentage contributions of 17.18%, 15.18%, 11.49% and 1.40%, respectively. When the interaction between every atom inside of Hirshfeld surface and an atom outside of Hirshfeld surface is also examined, it is discovered that the All···H interaction is the strongest interaction, contributing 59.60% percent of the total. The contributions of All···C, All···Cl, All···O and All···N were 15.60%, 12.80%, 10.80% and 1.20%, respectively (Supplementary Figure 1).

A void investigation is carried out as this analysis is directly related to the response of the single crystals to the applied stress as well as the strength of the crystal packing. The void computation is built on adding up the electronic density of the atoms that are supposed to be spherically symmetric [53–56]. According to the results of the present research, the void volume is calculated to be 168.26 $Å^3$, indicating that only 13.59% of the space in the unit cell is covered by voids (Fig. 7).

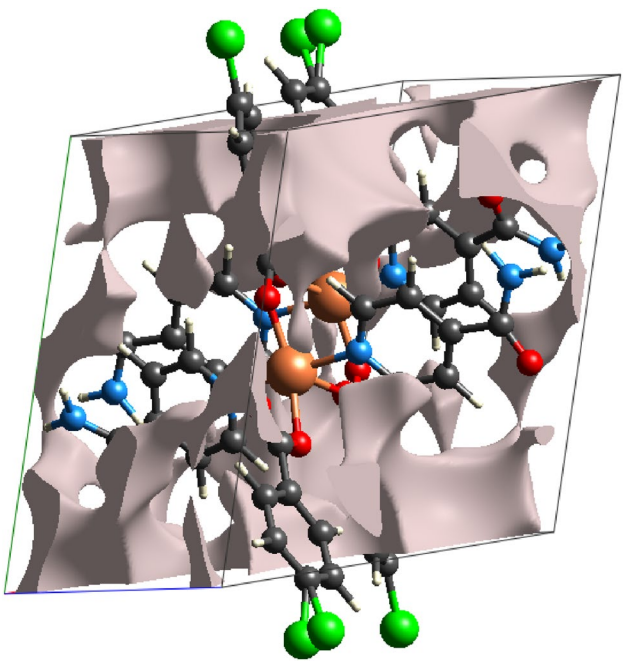

Fig. 7 Graphical representation of voids in the crystal packing for the complex

IR study

The vibrations of functional groups in the structure of the complex were determined by FTIR spectroscopy. The FTIR spectrum of the complex is given in Supplementary Figure 2. Asymmetric and symmetrical N–H vibrations of complexes containing isonicotinamide have been reported at 3300–3100 cm^{-1} [57–59]. N–H vibrations of the synthesized complexes in this study were observed at 3379–3163 cm^{-1}. The slight chemical shift in the symmetrical N–H vibration is due to N–H···O hydrogen bonds. Medium strong bands observed in the range of 3100–3000 cm^{-1} belong to aromatic C–H vibrations. According to the data in previous studies, the carboxamide group C=O vibration of the isonicotinamide ligand is observed at 1666 cm^{-1}. C=O vibration of the carboxamide group of the synthesized complex was observed at 1686 cm^{-1}. The absence of a chemical shift confirms that there is no coordination over the oxygen atoms of the carboxamide group to the metal atom. The 1700–1500 cm^{-1} region is complex due to the overlapping of the peaks of many functional groups in the structure of the complex. The reason why these bands are observed at lower wavelengths compared to free organic ligands is due to their interaction with metal atoms. Asymmetric COO^- and symmetrical COO^- vibrations of the complex were observed at 1571–1388 cm^{-1}, respectively. The $\Delta\upsilon$ value is calculated from the difference between asymmetric and symmetrical COO^- group vibrations. Compared to the sodium salt of the acid, this value indicates that if the sodium salt of the acid is greater than $\Delta\upsilon$ COO^-, the monodentate is attached to the metal atom of the carbonyl group, and if it is small, it indicates the formation of a bidentate or chelate [60]. $\Delta\upsilon$ values were calculated as 183 cm^{-1}, respectively. The $\Delta\upsilon$ value of the sodium salt of 4-chlorobenzoic acid is 200 cm^{-1} [61]. This value is higher than the value of the synthesized complex. Therefore, the results of the structure analysis determined by single-crystal X-ray diffraction and the results of FTIR spectra are in agreement, and as a result, the carboxylate oxygen atoms are coordinated to the metal atom as a bidentate bridge. C–N absorption bands in the pyridine ring of the isonicotinamide ligand were seen at 1030 cm^{-1}. The 1,4-disubstituted benzene vibration was detected at 857 cm^{-1} (1) for complex 1.

Electronic studies and fluorescence

The absorption spectra of the complex as measured by UV–Vis spectrophotometer are given in Supplementary Figure 3. The linear absorption spectrum gives information about energy band structures and forbidden energy gaps. When the linear absorption spectrum of the complex is examined, it is seen that it has Q bands around 753 nm assignable to $^2Eg \rightarrow {}^2T_2g$ transition, characteristic of

octahedral coordination of Cu(II) ion. Q bands consist of linear combinations of atomic orbital coefficients in the highest occupied molecular orbital [62, 63]. $n \rightarrow \pi^*$ or $\pi \rightarrow \pi^*$ transitions cause peaks due to the presence of Q bands in the linear absorption spectrum. C–N, C–Cl, C–O and C–H bonds in the structure of the complexes cause $n \rightarrow \sigma^*$ or $\sigma \rightarrow \sigma^*$ transitions. These bands in the linear absorption spectrum were seen at a wavelength of 282 nm.

The fluorescence spectra obtained when the complex are excited with a fluorescence spectrophotometer at a wavelength of 200–1100 nm are given in Supplementary Figure 4. The fluorescence intensities of the complex are given in Table 3.

It has been observed that the complex radiates in a broad spectrum in the wavelength range of about 350 – 550 nm. In addition, the complex radiates in the wavelength range of 750–770 nm. Due to these radiations, the complex is thought to have wide application potential in optics and optoelectronics. The radiations here are due to $\pi^* \rightarrow \pi$ and $\pi^* \rightarrow n$ transitions caused by functional groups such as benzene ring, pyridine ring, carboxylate, carboxamide and chlorine in the main and auxiliary ligands [64]. These complexes, which have fluorescent properties, can radiate; it is possible to use in optical and chemical sensors in detectors for biosensors, DNA quenching and nitroaromatic explosives [65, 66].

Anticancer and cytotoxic properties

There are no studies in the literature on the determination of the cytotoxicity of copper complexes with N-donor ligands on normal lymphocyte cells. In studies where anticancer properties were determined, the effects on healthy cell lines were not examined. The anticancer properties of the synthesized complex and its main and auxiliary ligands on DLD-1 colon cancer cells were investigated and compared with the starting ligands and solvent (DMSO). The cytotoxicity of the complex decreases with increasing concentration. The reference drug gemcitabine caused a decrease in cell viability as the concentration increased. Complex 1 caused more cell death than the reference drug at concentrations of 250 ppm and below. The complex also caused less cell death than the starting components 4-chlorobenzoic acid and isonicotinamide, but it was determined that the complex was moderately cytotoxic on the DLD-1 cell line (Supplementary Figure 5).

Table 3 Fluorescence intensity of the complex

Complex	Wavelength (nm)	Fluorescence intensity
1	381	158
	435	64
	756	12

The cytotoxic properties of the complex and its starting ligands on MCF-7 breast cancer cells were also investigated in this study. Complex 1 is not cytotoxic on MCF-7 cells. On the contrary, it was determined that the compound caused cell proliferation in the concentration range of 125–1000 ppm. In the 7.81–62.5 ppm concentration range, the complex is negligibly cytotoxic. Compared with the reference substance 5-fluorouracil (5-FU), the starting components of the complex, 4-chlorobenzoic acid and isonicotinamide, also cause mild cytotoxic effects on MCF-7 cells (Supplementary Figure 6).

The cytotoxic properties of the complex and its starting ligands on PC-3 prostate cancer cells were also investigated. Complex 1 is not cytotoxic on PC-3 cells. The complex caused cell proliferation at all concentrations studied. It was determined that proliferation increased with increasing concentration. The reference substance 5-fluorouracil caused a 40% decrease in cell viability. The starting components of the complex, 4-chlorobenzoic acid and isonicotinamide caused moderate cytotoxic effects on PC-3 cells (Supplementary Figure 7).

To recommend a compound as an anticancer drug, it is necessary to investigate not only its effects on cancer cells but also its effects on normal cells. Based on this, the cytotoxic effects of the synthesized complex and its starting components on human peripheral mononuclear blood cells (lymphocytes) were also investigated in this study. According to the results of the statistical analysis, there is a statistically significant difference between the results obtained at all concentrations examined for all cell lines. Complex 1, which has a moderate cytotoxic effect on DLD-1 cells, caused the proliferation in lymphocyte cells. In particular, it was determined that proliferation increased with increasing concentration in the concentration range of 500–31.25 ppm. It was determined that the complex was cytotoxic on lymphocyte cells at 15.62 and 7.81 ppm concentrations. However, it is possible to evaluate this as negligible toxicity according to international standards (Supplementary Fig. 8).

Molecular docking studies

Molecular docking is a bioinformatics method that allows estimating the interaction energy and interaction types when a ligand binds to another target molecule [33, 47, 48, 67–69]. When the interactions of the complex with the DNA molecule were examined, the binding energy was calculated as −7.1 kcal/mol. It was determined that strong hydrogen bond interactions with an average bond length of 2.64 Å were found between the complex with DA5, DA18 and DG4 base regions of DNA molecule. Also, it has been determined that there are carbon-hydrogen bond interactions between the

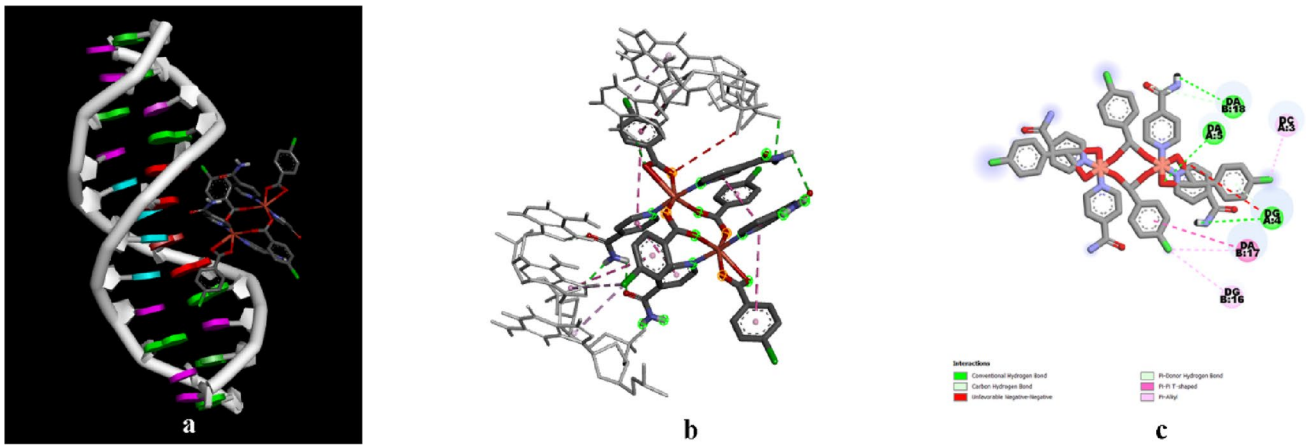

Fig. 8 **a** The molecular docking results of the complex with DNA molecule (1BNA). **b** Ligand–target interactions result between the complex and DNA molecule (1BNA). **c** 2D interactions of the complex with DNA molecule (1BNA)

complex and the DA18 base. Similarly, the complex molecule makes π-donor hydrogen bonds with the DG4 base region, π-π T-shaped interactions with the DG4 and DA17 bases and π-alkyl interactions with the DC3, DG16 and DA17 bases (Fig. 8).

Conclusion

In this study, the dimeric bis(μ-4-chlorobenzoato-κ^2O:O′) bis[(4-chlorobenzoato-κ^2O:O′-bis(isonicotinamide-κN) copper(II)] complex was synthesized. In the literature, there are only six structures similar to the crystal structure of this complex we have synthesized. Therefore, it is a compound with an unusual structure. It is recommended to be used in optical and optoelectronic applications due to the radiation in the wide wavelength range between 350 and 550 nm recorded in the fluorescence spectrum of the complex. The complex, which does not exhibit cytotoxic effects on healthy lymphocyte cells, is a good drug candidate. Although the complex showed weak anticarcinogenic effects on MCF-7 and PC-3 cancer cells, it exhibited a remarkable cytotoxic effect on DLD-1 cells. Thanks to its moderate cytotoxic effect, it is thought that complex has the potential of a non-platinum-based anticancer drug for colon cancer treatment. Docking results indicated that the compound had a strong affinity in binding to the DNA.

Supplementary Information The online version contains supplementary material available at https://doi.org/10.1007/s13738-022-02656-y.

Acknowledgements We are grateful to Prof. Dr. Bingür Sönmez, Prof. Dr. Fikrettin Şahin, Assoc. Prof. Dr. Özkan Özden, Fatih Ünal, Dr. Cem Öziç, Dr. Yunus Ensari, Didem Yıldırım and Yıldırım Öztürkkan for their support.

Declarations

Conflict of interest There is no conflict of interest to declare.

References

1. S. Ghosh, Bioorg. Chem. **88**, 102925 (2019)
2. S. Yadav, I. Yousuf, M. Usman, M. Ahmad, F. Arjmand, S. Tabassum, RSC Adv. **5**, 50673 (2015)
3. W.M. Al-Asbahy, M. Usman, F. Arjmand, M. Shamsi, S. Tabassum, Inorg. Chim. Acta. **445**, 167 (2016)
4. C.X. Zhang, S.J. Lippard, Curr. Opin. Chem. Biol. **7**, 481 (2003)
5. C. Marzano, M. Pellei, F. Tisato, C. Santini, ACAMC **9**, 185 (2009)
6. E. Vrontaki, G. Leonis, M.G. Papadopoulos, M. Simcic, S.G. Grdadolnik, A. Afantitis, G. Melagraki, S.K. Hadjikakou, T. Mavromoustakos, J. Chem. Inf. Model. **52**, 3293 (2012)
7. Z. Boulsourani, S. Katsamakas, G.D. Geromichalos, V. Psycharis, C.P. Raptopoulou, D. Hadjipavlou-Litina, E. Yiannaki, C. Dendrinou-Samara, Mater. Sci. Eng. C **76**, 1026 (2017)
8. M.J. Hannon, Pure Appl. Chem. **79**, 2243 (2007)
9. B.A. Teicher, P.A. Andrews (eds.), *Anticancer Drug Development Guide: Preclinical Screening, Clinical Trials, and Approval*, 2nd edn. (Humana Press, Totowa, 2004)
10. C. Acilan, B. Cevatemre, Z. Adiguzel, D. Karakas, E. Ulukaya, N. Ribeiro, I. Correia, J.C. Pessoa, Biochim. Biophys. Acta (BBA) Gen. Subj **1861**, 218 (2017)
11. R.R. Crichton, *Biological Inorganic Chemistry: An Introduction*, 1st edn. (Elsevier, Amsterdam, 2008)
12. B. Tunçsoy, S. Sugeçti, E. Büyükgüzel, P. Özalp, K. Büyükgüzel, Bull. Environ. Contam. Toxicol. **107**, 412 (2021)
13. J. Easmon, G. Pürstinger, G. Heinisch, T. Roth, H.H. Fiebig, W. Holzer, W. Jäger, M. Jenny, J. Hofmann, J. Med. Chem. **44**, 2164 (2001)
14. M. Barceló-Oliver, Á. García-Raso, Á. Terrón, E. Molins, M.J. Prieto, V. Moreno, J. Martínez, V. Lladó, I. López, A. Gutiérrez, P.V. Escribá, J. Inorg. Biochem. **101**, 649 (2007)
15. S. Chernomorsky, R. Rancourt, K. Virdi, A. Segelman, R.D. Poretz, Cancer Lett. **120**, 141 (1997)
16. L. Tabrizi, D.Q. Dao, T.A. Vu, RSC Adv. **9**, 3320 (2019)

17. H. Zhou, C. Zheng, G. Zou, D. Tao, J. Gong, Int. J. Biochem. Cell. Biol. **34**, 678 (2002)
18. F. Gomes da Silva Dantas, A. Araújo de Almeida-Apolonio, R. Pires de Araújo, L. Regiane Vizolli Favarin, P. Fukuda de Castilho, F. De Oliveira Galvão, T. Inez Estivalet Svidzinski, G. Antônio Casagrande, K. Mari Pires de Oliveira, Molecules **23**, 1856 (2018)
19. M. Geraghty, J.F. Cronin, M. Devereux, M. McCann, Biometals **13**, 1 (2000)
20. D.A. da Silva, A. De Luca, R. Squitti, M. Rongioletti, L. Rossi, C.M.L. Machado, G. Cerchiaro, J. Inorg. Biochem. **226**, 111634 (2022)
21. N.K. Singh, A.A. Kumbhar, Y.R. Pokharel, P.N. Yadav, J. Inorg. Biochem. **210**, 111134 (2020)
22. M. Devereux, D. O'Shea, M. O'Connor, H. Grehan, G. Connor, M. McCann, G. Rosair, F. Lyng, A. Kellett, M. Walsh, D. Egan, B. Thati, Polyhedron **26**, 4073 (2007)
23. M. Devereux, M. McCann, D.O. Shea, R. Kelly, D. Egan, C. Deegan, K. Kavanagh, V. McKee, G. Finn, J. Inorg. Biochem. **98**, 1023 (2004)
24. M. Devereux, M. McCann, D. O'Shea, M. O'Connor, E. Kiely, V. McKee, D. Naughton, A. Fisher, A. Kellett, M. Walsh, D. Egan, C. Deegan, Bioinorg. Chem. Appl. **2006**, 80283 (2006)
25. K.N. Aneesrahman, K. Ramaiah, G. Rohini, G.P. Stefy, N.S.P. Bhuvanesh, A. Sreekanth, Inorg. Chim. Acta. **492**, 131 (2019)
26. M.C. Rodríguez-Argüelles, A. Sánchez, M. Belicchi Ferrari, G. Gasparri Fava, C. Pelizzi, G. Pelosi, R. Albertini, P. Lunghi, S. Pinelli, J. Inorg. Biochem. **73**, 7 (1999)
27. D. Rogolino, A. Cavazzoni, A. Gatti, M. Tegoni, G. Pelosi, V. Verdolino, C. Fumarola, D. Cretella, P.G. Petronini, M. Carcelli, Eur. J. Med. Chem. **128**, 140 (2017)
28. D. Bruker, *APEX2, SAINT and SADABS* (Bruker AXS Inc., Madison, 2012)
29. G.M. Sheldrick, Acta Crystallogr. A Found. Adv. **64**, 112 (2008)
30. L.J. Farrugia, J. Appl. Crystallogr. **45**, 849 (2012)
31. A.L. Spek, Acta. Crystallogr. D Biol. Crystallogr. **65**, 148 (2009)
32. F.L. Hirshfeld, Theor. Chim. Acta. **44**, 129 (1977)
33. M.A. Spackman, D. Jayatilaka, CrystEngComm **11**, 19 (2009)
34. P.R. Spackman, M.J. Turner, J.J. McKinnon, S.K. Wolff, D.J. Grimwood, D. Jayatilaka, M.A. Spackman, J. Appl. Crystallogr. **54**, 1006 (2021)
35. J. J. McKinnon, D. Jayatilaka, and M. A. Spackman, Chem. Commun. 3814 (2007).
36. T. Mosmann, J. Immunol. Methods. **65**, 55 (1983)
37. O. Trott, A.J. Olson, J. Comput. Chem. NA (2009)
38. H.R. Drew, R.M. Wing, T. Takano, C. Broka, S. Tanaka, K. Itakura, R.E. Dickerson, Proc. Natl. Acad. Sci. **78**, 2179 (1981)
39. BIOVIA, Dassault Systèmes, *BIOVA Discovery Studio Visualizer 2021, v21.1.0.20298* (Dassault Systèmes, San Diego, 2021)
40. T. Hökelek, V. Yavuz, H. Dal, H. Necefoğlu, Acta Crystallogr. E Crystallogr. Commun. **74**, 45 (2018)
41. H. Necefoğlu, T. Hökelek, C.C. Ersanlı, A. Erdönmez, Acta Crystallogr. E Crystallogr. Commun. **58**, m758 (2002)
42. T. Hökelek, N. Çaylak, H. Necefoğlu, Acta Crystallogr. E Crystallogr. Commun. **64**, m505 (2008)
43. T. Hökelek, H. Dal, B. Tercan, F.E. Özbek, H. Necefoğlu, Acta Crystallogr. E Crystallogr. Commun. **65**, m607 (2009)
44. T. Hökelek, H. Necefouglu, Acta Crystallogr. C Cryst. Struct. Commun. **52**, 1128 (1996)
45. T. Hökelek, H. Dal, B. Tercan, Ö. Aybirdi, H. Necefoğlu, Acta Crystallogr. E Crystallogr. Commun. **65**, m651 (2009)
46. T. Hökelek, F. Yılmaz, B. Tercan, F. Gürgen, H. Necefoğlu, Acta Crystallogr. E Crystallogr. Commun. **65**, m1416 (2009)
47. F. Greenaway, A. Pezeshk, A. Cordes, M. Noble, J. Sorenson, Inorg. Chim. Acta **93**, 67 (1984)
48. H. Kargar, M. Fallah-Mehrjardi, R. Behjatmanesh-Ardakani, K.S. Munawar, M. Ashfaq, M.N. Tahir, J. Mol. Struct. **1241**, 130653 (2021)
49. H. Kargar, M. Bazrafshan, M. Fallah-Mehrjardi, R. Behjatmanesh-Ardakani, H.A. Rudbari, K.S. Munawar, M. Ashfaq, M.N. Tahir, Polyhedron **202**, 115194 (2021)
50. H. Kargar, M. Fallah-Mehrjardi, R. Behjatmanesh-Ardakani, K.S. Munawar, M. Ashfaq, M.N. Tahir, Polyhedron **208**, 115428 (2021)
51. H. Kargar, M. Fallah-Mehrjardi, M. Ashfaq, K.S. Munawar, M.N. Tahir, R. Behjatmanesh-Ardakani, H. Amiri Rudbari, A. Adabi Ardakani, S. Sedighi-Khavidak, J. Coord. Chem. **74**, 2720 (2021)
52. H. Kargar, M. Fallah-Mehrjardi, R. Behjatmanesh-Ardakani, K.S. Munawar, M. Ashfaq, M.N. Tahir, Inorg. Chim. Acta **526**, 120535 (2021)
53. A. Jamshidvand, M. Sahihi, V. Mirkhani, M. Moghadam, I. Mohammadpoor-Baltork, S. Tangestaninejad, H. Amiri Rudbari, H. Kargar, R. Keshavarzi, S. Gharaghani, J. Mol. Liq. **253**, 61 (2018)
54. H. Kargar, R. Behjatmanesh-Ardakani, V. Torabi, A. Sarvian, Z. Kazemi, Z. Chavoshpour-Natanzi, V. Mirkhani, A. Sahraei, M. Nawaz Tahir, M. Ashfaq, Inorg. Chim. Acta. **514**, 120004 (2021)
55. H. Kargar, R. Behjatmanesh-Ardakani, V. Torabi, M. Kashani, Z. Chavoshpour-Natanzi, Z. Kazemi, V. Mirkhani, A. Sahraei, M.N. Tahir, M. Ashfaq, K.S. Munawar, Polyhedron **195**, 114988 (2021)
56. H. Kargar, M. Ashfaq, M. Fallah-Mehrjardi, R. Behjatmanesh-Ardakani, K.S. Munawar, M.N. Tahir, J. Mol. Struct. **1253**, 132264 (2022)
57. L.J. Bellamy, *The Infrared Spectra of Complex Molecules. Vol. 1*. Aufl., Repr (Chapman and Hall, London, 1986).
58. P.J. Larkin, *Infrared and Raman Spectroscopy: Principles and Spectral Interpretation* (Elsevier, Amsterdam, 2011)
59. M. Huseynova, V. Farzaliyev, A. Medjidov, M. Aliyeva, M. Özdemir, P. Taslimi, Y. Zorlu, B. Yalçın, O. Şahin, J. Mol. Struct. **1248**, 131470 (2022)
60. K. Nakamoto, *Infrared and Raman Spectra of Inorganic and Coordination Compounds*, 4th edn. (Wiley, New York, 1986)
61. E.F. Öztürkkan, D.A. Köse, H. Necefoglu, I. Uzun, Asian J. Chem. **19**, 9 (2007)
62. A. Mandal, B.K. Patel, Polyhedron **132**, 112 (2017)
63. D. Dimić, C. R. Chim. **21**, 1001 (2018)
64. L. Basabe-Desmonts, D.N. Reinhoudt, M. Crego-Calama, Chem. Soc. Rev. **36**, 993 (2007)
65. J. R. Lakowicz, *Principles of Fluorescence Spectroscopy*, 3 edn, corrected at 4. printing (Springer, New York, 2010).
66. T. Caron, M. Guillemot, F. Veignal, P. Montméat, E. Pasquinet, P. Prené, F. Perraut, J. Lère-Porte, F. Serein-Spirau, M. Pardo, and G. Sberveglieri, in *AIP Conference Proceedings* (AIP, Brescia, 2009), pp. 83–85
67. R.R. Narkhede, R.S. Cheke, J.P. Ambhore, S.D. Shinde, Euroasian J Med. Oncol. **4**, 185–195 (2020)
68. S. Singh, H. Florez, F1000Res **9**, 502 (2020)
69. G.M. Morris, M. Lim-Wilby, Methods Mol. Biol. **443**, 365 (2008)